First results from the Madison Symmetric Torus reversed field pinch*

S. C. Prager,† A. F. Almagri, S. Assadi, J. A. Beckstead, R. N. Dexter,
D. J. Den Hartog, G. Chartas, S. A. Hokin, T. W. Lovell, T. D. Rempel, J. S. Sarff,
W. Shen, C. W. Spragins, and J. C. Sprott
Department of Physics, University of Wisconsin, Madison, Wisconsin 53706

(Received 5 December 1989; accepted 21 February 1990)

The first period of physics operation of the Madison Symmetric Torus (MST) reversed field pinch [*Plasma Physics and Controlled Nuclear Fusion Research 1988* (IAEA, Vienna, 1989), Vol 2, p. 757] has produced information on sawtooth oscillations, edge magnetic and electrostatic fluctuations, and equilibrium parameters at large plasma size. Sawtooth oscillations are prevalent at all values of pinch parameter and might constitute discrete dynamo events. Both electrostatic and magnetic fluctuations are of sufficient magnitude to be relevant to transport in the reversed field pinch. In the plasmas studied to date (up to a plasma current of 0.5 MA) the poloidal beta value is about 10% or greater.

I. INTRODUCTION

The Madison Symmetric Torus (MST) is a new reversed field pinch (RFP) experiment that recently began operation.[1] MST is large in size (0.52 m minor radius and 1.5 m major radius) and moderate in plasma current (<1 MA capability). The physics goals for the first several years of operation will be twofold: first, to investigate turbulence and transport, as it pertains specifically to the RFP and to toroidal confinement, in general; and second, to ascertain the effect of large plasma size on RFP confinement.

Here we describe a variety of experimental results obtained during the first period of physics operation of MST. Following a brief description of the device and plasma parameters (Sec. II), we present observations of sawtooth oscillations (Sec. III). These oscillations are especially vivid in MST and provide insight into magnetic reconnection and dynamo activity in the RFP. In Sec. IV we describe initial observations of edge magnetic and electrostatic oscillations, and in Sec. V we conclude with comments on the relation of achieved MST plasma parameters to projections toward a reactor.

II. MACHINE DESCRIPTION AND PLASMA PARAMETERS

The design of MST was driven by the desire for small field errors and efficient machine disassembly. A 5 cm thick aluminum torus serves as vacuum vessel, toroidal field winding (by driving poloidal current through the vessel), and stabilizing shell. The poloidal field winding is placed around the 2.0 Wb iron core. The absence of field windings surrounding the device facilitates machine disassembly and diagnostic access. The single-turn toroidal field concept also yields a small field ripple; the radial field that enters the toroidal gap produces, in the absence of plasma, a dominant Fourier component of $m=0, n=4$ with a magnitude of about 0.2% of the equilibrium toroidal field. The field error at the poloidal gap is reduced by a special flange. A winding used to reverse bias the iron core is distributed so as to limit the dc error field within the plasma to less than 1 G. A full description of the somewhat complicated poloidal field system, and other machine features, is provided in Ref. 2. For the results reported here, the final poloidal field winding was not yet installed. The bias winding served as the Ohmic heating coil, with the result that the pulsed field errors accompanying this temporary setup are significant. The vessel is pumped through an array of 193 3.8 cm diam holes in order to provide very high pumping speed while eliminating the deeply penetrating field errors that would otherwise be produced by large pump ports.

Table I lists the plasma parameters achieved during the first seven month period of physics operation. Also listed are the projected parameters anticipated from optimistic scaling from present devices (i.e., assuming classical resistivity scaling and constant beta scaling). The full parameter capability of MST awaits further plasma optimization through field error reduction, loop voltage programming, etc. Plasma current of 0.5 MA is produced at a toroidal loop voltage of 30 V (startup requires 150 V). The discharge is sustained for about 35 msec as the plasma evolves along an F-θ trajectory as observed in other RFP experiments. The central electron temperature is about 350 eV (measured by Thomson scattering at $I_p = 0.44$ MA). The central density is typically 2×10^{13} cm^{-3}, twice the line-averaged density. The energy

TABLE I. MST plasma parameters.

	Achieved (optimistic projection)
I_p	0.5 MA (1 MA)
V_L	30 V (4 V)
Volt-seconds	1.4 (<2 available)
Pulse length	35 msec
τ_E	1 msec (10 msec)
τ_ρ	0.6 msec
$T_e(0)$	0.35 keV (1 keV) (@0.44 MA)
$n_e(0)$	2×10^{13} cm^{-3}
$\langle B_T\rangle$	1.2 kG
β_P	$\approx 10\%$

* Paper 4I3, Bull. Am. Phys. Soc. **34**, 2000 (1989).
† Invited speaker.

 0899-8221/90/061367-05$02.00

confinement time is roughly 1 msec and the poloidal beta is roughly 10%.

III. SAWTOOTH OSCILLATIONS

In both the tokamak[3] and reversed field pinch,[4–7] sawtooth oscillations occur in magnetic field and plasma energy. In both configurations, the sawtooth oscillation is usually interpreted as a sudden magnetic reconnection described by resistive magnetohydrodynamics (MHD), with $m = 1$ modes playing a dominant role. There are, however, significant differences in the details of reconnection in the two cases, as a result of the different q profiles. In MST, sawteeth are particularly vivid and prevalent. They occur at all values of θ, where the pinch parameter, $\theta = B_p(a)/\langle B_T \rangle$, is the ratio of the poloidal magnetic field at the plasma edge to the average toroidal field (toroidal flux divided by cross-sectional area). This is in contrast to other experiments, such as ZT-40M,[4–6] in which they occur mainly at high values of θ.

Although the plasma current varies smoothly, the toroidal magnetic flux within the shell contains inverted sawteeth and the toroidal field at the wall contains sawteeth, as shown in Fig. 1. Interestingly, $B_T(a)$ is at all times increasing toward zero, *except* during the crash phase. It is only during the crash that $B_T(a)$ is negative-going, corresponding to the generation of reversed field. Thus the sawtooth crash might constitute discrete dynamo events.[4] As in ZT-40M, the sawtooth trajectory (Fig. 2) in F-θ space [where the field reversal parameter $F = B_T(a)/\langle B_T \rangle$] indicates that the sawtooth crash carries the plasma closer to the minimum energy Taylor state,[6] which lies to the left of the origin of the figure. As in a tokamak, the sawtooth relaxation likely corresponds to a sudden flattening of the current density profile. This is indicated in Fig. 1 by the asymmetry factor, $\Lambda = \beta_p + l_i - 1$ (where l_i is the internal inductance), obtained from the measured edge poloidal magnetic field $B_p = 1 + \epsilon\Lambda \cos\theta$ (where ϵ is the inverse aspect ratio). The time evolution of Λ

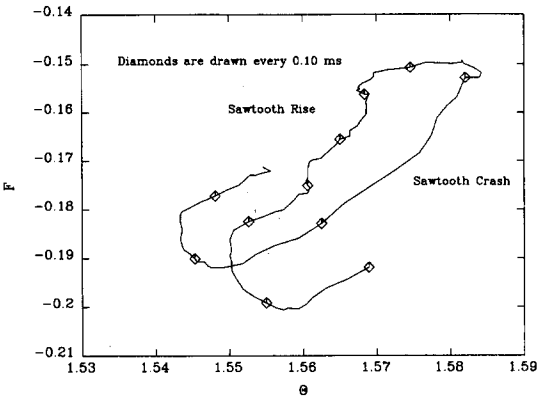

FIG. 2. Trajectory of a sawtooth oscillation in F-θ space.

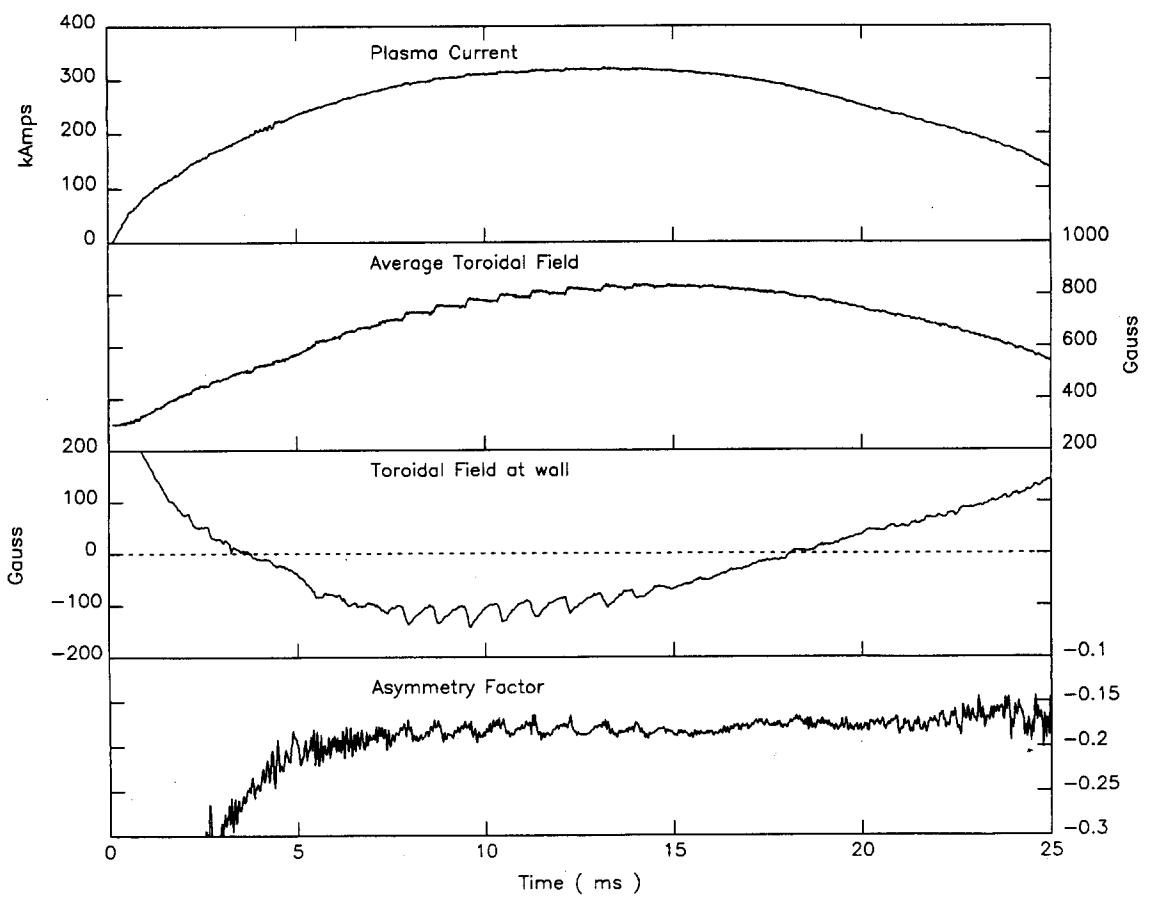

FIG. 1. Time dependence of plasma current, toroidal magnetic flux within the shell, toroidal magnetic field at the wall, and edge poloidal field asymmetry factor. Sawtooth oscillations are illustrated.

indicates a slow peaking of the current density during the rise phase of sawtooth, followed by the sudden flattening. Also similar to the tokamak sawtooth is the redistribution of plasma energy from the core to the edge, as illustrated by the soft x-ray emissivity as seen from a central and edge chord (Fig. 3). The redistribution is indicated in many measurements; e.g., the line-averaged density displays sawtooth oscillations, whereas the edge density, measured by visible radiation and Langmuir probes, displays inverted sawteeth. The inversion radius for the soft x-ray sawteeth is about 35 cm, which is about $0.7a$. Thus the RFP inversion radius is much greater than the typical tokamak sawtooth inversion radius, implying that the reconnection in the RFP might be more global than in the tokamak. Such might be expected from a simple comparison of the $m = 1$ linear eigenfunctions. In a tokamak, the $m = 1$ resistive internal kink is localized within the $q = 1$ surface, whereas in a RFP the $m = 1$ displacement extends over the entire radius.[8]

Oscillations at roughly 15 kHz sometimes precede the sawtooth crash. These precursor oscillations, observed in the edge magnetic field and in soft x-ray signals, have poloidal and toroidal mode numbers that are dominantly $m = 1, n \approx -6$. These mode numbers correspond to a disturbance that is resonant inside the reversal surface. From linear theory, the toroidal mode number is expected to be proportional to the aspect ratio, R/a. Indeed, comparing precursors in MST with those in ZT-40M, we observe the expected aspect ratio dependence; in ZT-40M, with an aspect ratio twice that of MST, n is typically between 8 and 15.[5]

Recently, a MHD computation at very low aspect ratio (1.6), by Kusano and Sato,[9] has produced sawtooth oscillations in magnetic quantities, such as reversal parameter F, which qualitatively resemble the experimental results in MST. In the computation, both $m = 0$ and $m = 1$ helical modes occur during the crash. The toroidal mode number of the $m = 1$ mode is $n = 2R/a$. For MST, with $R/a = 3$, we expect $n = 6$, as is observed for the precursor oscillations. However, the computation suggests that significant modal activity accompanies the crash. A burst in $m = 0$ edge magnetic field accompanies the crash in MST, but details await further measurements.

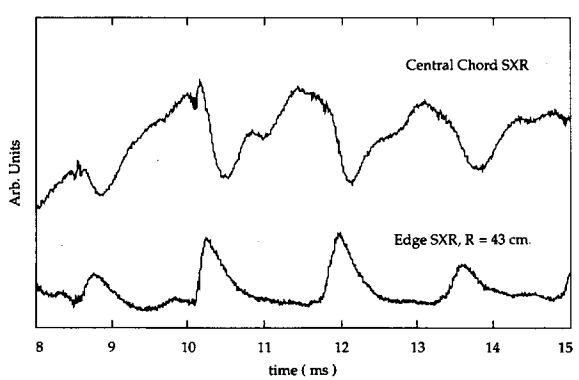

FIG. 3. Soft x-ray emissivity viewed from a chord passing through the center and a chord at the edge ($r = 43$ cm).

Finally, there are two conjectures for why sawteeth are more pervasive in MST than in other RFP's. First, the relatively low aspect ratio of MST encourages sawteeth. At low aspect ratio, helical modes are well separated in wavelength and must grow to large amplitude for the onset of the nonlinear coupling that might then produce large sawteeth. This interpretation is suggested by the computation of Ref. 9 in which a run with higher aspect ratio (4.8) produced very small sawteeth and more continuous dynamo generation of reversal. Second, sawteeth in the experiment often occur mainly during the first half of the discharge as the current is rising and the surface loop voltage is quite large. Thus the prevalence of sawteeth might be a result of the imperfect flattop of the discharge. Perhaps the time variation produces a relatively peaked current density distribution that favors sawteeth. Improved voltage programming will test this speculation.

IV. EDGE FLUCTUATIONS

A. Magnetic fluctuations

Magnetic fluctuations in RFP's have relatively large amplitude. The measured mode numbers of the edge magnetic fluctuations indicate that the modes are resonant inside the reversal surface, as expected for resistive MHD modes that are predicted to produce the dynamo effect. However, the sawtooth oscillations described above suggest the possibility that the dynamo effect in some discharges might only occur during the sawtooth crash. The magnetic fluctuations might not be fully, or partially, produced by the dynamo modes. For example, resistive interchange and electromagnetic drift wave turbulence might be active in the RFP.

In MST, initial observation of edge magnetic fluctuations are in general agreement with measurements in smaller devices.[10] The amplitude of edge magnetic fluctuations (of wavelengths exceeding several centimeters) is about 1%. The fluctuation power decays with frequency, with about 90% of the power concentrated below 30 kHz. The amplitude of the toroidal field fluctuation is roughly twice that of the poloidal field. However, at high frequency the fluctuation amplitude is directed mainly perpendicular to the equilibrium field. For example, excluding frequencies below 25 kHz, the toroidal field fluctuation is ten times larger than the poloidal field fluctuation. Such a polarization is as expected, for example, for incompressible drift waves at beta less than unity. However, the polarization is different than that of HBTX-1A,[10] in which the poloidal and toroidal field fluctuations are comparable at all frequencies investigated. Initial determination of the poloidal wavenumber spectrum from two-point measurements indicates that most of the fluctuation power would correspond to $m = 0$ and $m = 1$ modes, as seen previously. However, at high frequency the spectrum is broadened, as might be expected from nonlinear mode coupling. In the range of 150–250 kHz the power of the $m = 3$ mode is comparable to that of $m = 1$ fluctuations.

As in virtually all past RFP experiments, the magnetic fluctuations decrease upon reversal and minimize at zero or shallow reversal (at F about -0.1). Similarly, many measures of plasma quality, such as resistance, are optimal at

shallow reversal. The link between magnetic fluctuations and transport in MST, and RFP's in general, remains to be established. In MST, the quasilinear estimate of thermal transport, using the edge magnetic fluctuation amplitude and assuming the parallel correlation of an order of the minor radius, yields an energy confinement time comparable to that measured. In addition, magnetic fluctuations and energy confinement time sometimes vary together. For example, as a small paddle limiter is inserted into the plasma, the magnetic fluctuations and energy loss rate both decrease with insertion for the first 4 cm from the wall, and thereafter both increase with deeper penetration (Fig. 4). Although these results are suggestive, there are also indications of other loss channels; for example, modeling with a one-dimensional neutral particle transport code, combined with bolometry and H_α radiation measurements, suggests that charge exchange loss is also significant.

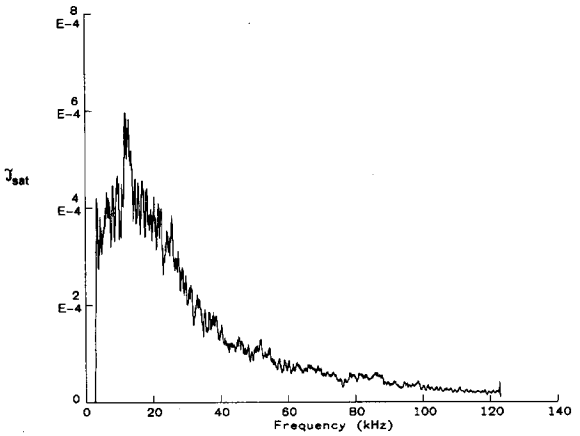

FIG. 5. Frequency spectrum of electrostatic fluctuations measured at the edge (0.7 cm from wall) by ion saturation current collected by a Langmuir probe.

B. Electrostatic fluctuations

The focus of RFP research on MHD and magnetic fluctuations has led to the relative neglect of electrostatic fluctuations. However, the electrostatic turbulence models of accepted importance to tokamak confinement might be similarly influential to RFP behavior. Initial measurements of edge fluctuations measured with Langmuir probes in MST, as shown in Fig. 5, indicate that such fluctuations are indeed of large amplitude (10%–20%) with a spectrum that mostly decays with frequency, as in a tokamak. As the reversal parameter F is varied, the fluctuations minimize at shallow reversal, as shown in Fig. 6. This F dependence is similar to that of the magnetic fluctuations (Fig. 6) and many confinement parameters, and raises the possibility that electrostatic and magnetic fluctuations are coupled. As a stimulus for further study of electrostatic fluctuations, we can evaluate the fluctuation-driven particle and energy convection. To interpret the probe measurements we assume, without validation at this point, that the temperature fluctuations are small. Then, fluctuations in ion saturation current may be interpreted as density fluctuations, and fluctuations in floating potential gradient (obtained from two probe tips) may be interpreted as electric field fluctuations. Assuming poloidal symmetry in the fluctuations, we may then obtain upper bounds in the convective flux of particles ($\Gamma = nE_T/B_p$) and energy ($\Gamma_E = 5\Gamma T_e/2$) arising from fluctuations. These estimates represent bounds on transport since we have not yet measured correlation between fluctuating quantities. These bounds predict that the particle confinement time should exceed 0.2 msec and the energy confinement time should exceed 0.5 msec. Both of these bounds are consistent with global measurements, and encourage future study.

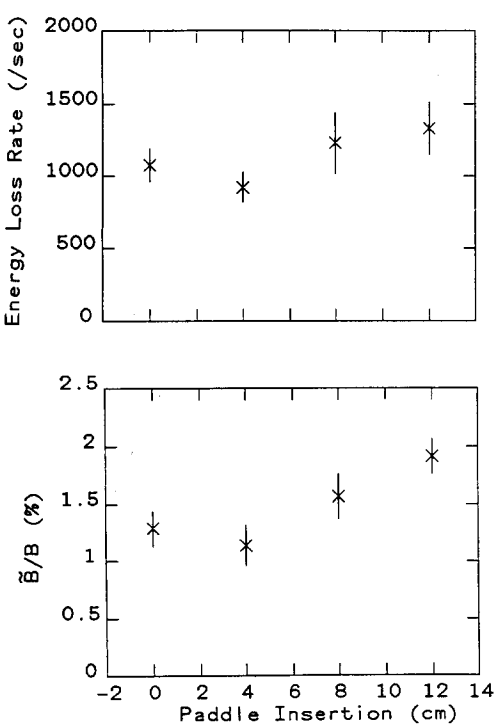

FIG. 4. Energy loss rate (τ_E^{-1}) and magnetic field fluctuation amplitude versus depth of insertion of paddle limiter, measured in centimeters from the wall.

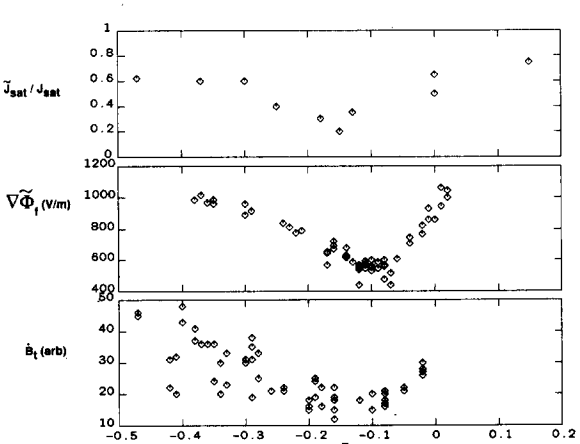

FIG. 6. Field reversal dependence of electrostatic fluctuations (ion saturation current and gradient in floating potential), and magnetic fluctuations (time derivative of toroidal magnetic field).

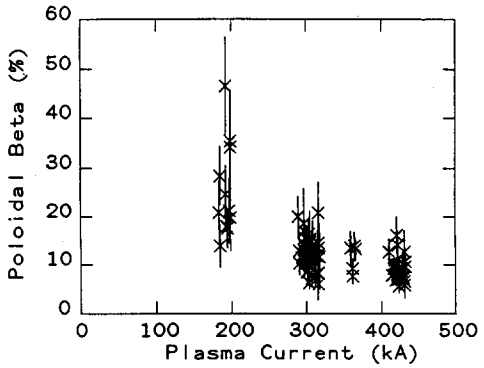

FIG. 7. Dependence of poloidal beta on plasma current. The scattering in the data results from statistical uncertainty of the Thomson scattering diagnostic.

V. CONCLUSIONS

The first period of physics operation of MST has indicated the possible importance of sawtooth oscillations, magnetic fluctuations, and electrostatic fluctuations to the behavior of a large RFP. Sawtooth oscillations occur at all values of pinch parameter. For most discharges, the toroidal field at the wall is increasing at all times except during the crash phase. Thus for these discharges the dynamo field generation might occur only during these discrete events. Magnetic fluctuations, as in past RFP experiments, are of sufficient magnitude to be relevant to transport. However, edge electrostatic fluctuations are also sufficiently large that their effect on particle and energy convection might be important and warrants serious investigation.

Although this initial operation of MST is far from optimized, the parameters achieved already have some implication for RFP behavior at large size. In MST, a plasma current of 0.5 MA is obtained with a volt-second consumption of about 1.4 Wb. This implies that the comparably sized RFX device at Padua[11] and ZTH device at Los Alamos[12] will very likely attain their design current values of 2 and 4 MA, respectively. Both devices are under construction and have roughly ten times the volt-second capability of MST.

All past RFP devices have operated with poloidal beta values of order 10%. If beta is assumed to be constant for all RFP devices, a rather favorable parameter scaling results. A key question is whether the high value of beta is maintained as the plasma size is increased. The answer from MST, up to a current level of 0.5 MA is yes, as illustrated in Fig. 7. Activity over the next year of MST operation will focus on (1) parameter optimization through, for example, field error reduction (through the installation of the permanent poloidal field winding) and flattopping (through improved voltage programming), (2) detailed investigation of edge electrostatic and magnetic turbulence (using 400 pickup coils installed within the vacuum on the surface of the vacuum vessel), and their correlation with transport and beta, and (3) the role of energetic electrons and anomalous ion heating.

ACKNOWLEDGMENT

This work has been supported by the U.S. Department of Energy.

[1] A. F. Almagri, S. Assadi, J. A. Beckstead, G. Chartas, D. J. Den Hartog, X. Deng, R. N. Dexter, S. A. Hokin, E. Hotta, D. W. Kerst, D. Kortbawi, J. Laufenberg, T. W. Lovell, E. J. Nilles, S. C. Prager, T. D. Rempel, J. S. Sarff, W. Shen, C. W. Spragins, and J. C. Sprott, in *Plasma Physics and Controlled Nuclear Fusion Research 1988,* Nice (IAEA, Vienna, 1989), Vol. 2, p. 757.
[2] R. N. Dexter, D. W. Kerst, T. W. Lovell, S. C. Prager, and J. C. Sprott, Fusion Technol. (in press).
[3] See, for example, G. L. Jahns, M. Soler, B. V. Waddell, J. D. Callen, and H. R. Hicks, Nucl. Fusion **18**, 609 (1978).
[4] R. G. Watt and R. A. Nebel, Phys. Fluids **26**, 1168 (1983).
[5] G. A. Wurden, Phys. Fluids **27**, 551 (1984).
[6] R. G. Watt and E. M. Little, Phys. Fluids **27**, 784 (1984).
[7] H. Y. W. Tsui and J. Cunnane, Plasma Phys. Controlled Fusion **30**, 865 (1988).
[8] See, for example, E. J. Caramana, R. A. Nebel, and D. D. Schnack, Phys. Fluids **26**, 1305 (1983).
[9] K. Kusano and T. Sato, submitted to Nucl. Fusion.
[10] See, for example, I. H. Hutchinson, M. Malacarne, P. Noonan, and D. Brotherton-Ratcliffe, Nucl. Fusion **24**, 59 (1984).
[11] G. Malesani, in *Proceedings of the International School of Plasma Physics, Workshop on Physics of Mirrors, Reversed Field Pinches and Compact Tori,* Varenna, Italy (Societa Italiana Di Fisica, Bologna, Italy, 1987), Vol. 1, p. 331.
[12] H. Dreicer, in Ref. 11, p. 359.